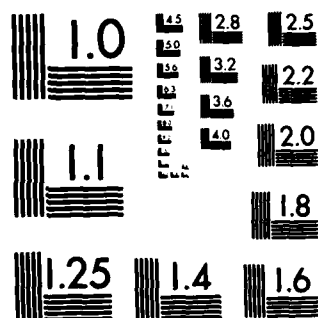


AD-A148 626 ACCELERATION OF AN ELECTRON RING IN A MODIFIED BETATRON 1/1  
WITH TRANSVERSE PRESSURE(U) NAVAL RESEARCH LAB  
WASHINGTON DC J M GROSSMAN ET AL. 86 DEC 84  
UNCLASSIFIED NRL-MR-5444 F/G 28/7 NL

								END					
								FILMED					
								DTIC					



MICROCOPY RESOLUTION TEST CHART  
NATIONAL BUREAU OF STANDARDS-1963-A

AD-A148 626

2

NRL Memorandum Report 5444

## Acceleration of an Electron Ring in a Modified Betatron with Transverse Pressure

J. M. GROSSMANN,\* J. M. FINN,\*\* AND W. M. MANHEIMER

*Plasma Theory Branch  
Plasma Physics Division*

*\*NRC-NRL Postdoctoral Associate*

*\*\*Laboratory for Plasma and Fusion Energy Research  
University of Maryland  
College Park, MD 20742*

December 6, 1984

This work was supported by the Office of Naval Research.



DTIC  
ELECTE  
DEC 18 1984  
S B D

NAVAL RESEARCH LABORATORY  
Washington, D.C.

Approved for public release; distribution unlimited.

84 12 07 009

DTIC FILE COPY

REPORT DOCUMENTATION PAGE					
1a REPORT SECURITY CLASSIFICATION <b>UNCLASSIFIED</b>			1b RESTRICTIVE MARKINGS		
2a SECURITY CLASSIFICATION AUTHORITY			3 DISTRIBUTION/AVAILABILITY OF REPORT		
2b DECLASSIFICATION/DOWNGRADING SCHEDULE			Approved for public release; distribution unlimited.		
4 PERFORMING ORGANIZATION REPORT NUMBER(S) <b>NRL Memorandum Report 5444</b>			5 MONITORING ORGANIZATION REPORT NUMBER(S)		
6a NAME OF PERFORMING ORGANIZATION <b>Naval Research Laboratory</b>		6b OFFICE SYMBOL (if applicable) <b>Code 4790</b>		7a NAME OF MONITORING ORGANIZATION	
6c ADDRESS (City, State, and ZIP Code) <b>Washington, DC 20375-5000</b>			7b ADDRESS (City, State, and ZIP Code)		
8a NAME OF FUNDING/SPONSORING ORGANIZATION <b>Office of Naval Research</b>		8b OFFICE SYMBOL (if applicable)		9. PROCUREMENT INSTRUMENT IDENTIFICATION NUMBER	
8c ADDRESS (City, State, and ZIP Code) <b>Arlington, VA 22217</b>			10 SOURCE OF FUNDING NUMBERS		
			PROGRAM ELEMENT NO <b>61153N</b>	PROJECT NO	TASK NO. <b>RR022-09-4E</b> WORK UNIT ACCESSION NO <b>DN180-207</b>
11 TITLE (Include Security Classification) <b>Acceleration of an Electron Ring in a Modified Betatron with Transverse Pressure</b>					
12 PERSONAL AUTHOR(S) <b>Grossmann, J.M.,* Finn, J.M.,** and Manheimer, W.M.</b>					
13a TYPE OF REPORT <b>Interim</b>		13b TIME COVERED FROM _____ TO _____		14 DATE OF REPORT (Year, Month, Day) <b>1984 December 6</b>	
15 PAGE COUNT <b>35</b>					
16 SUPPLEMENTARY NOTATION <b>*NRC-NRL Postdoctoral Associate</b> (Continues) <b>**Laboratory for Plasma and Fusion Energy Research, University of MD, College Park, MD 20742</b>					
17 COSATI CODES			18 SUBJECT TERMS (Continue on reverse if necessary and identify by block number)		
FIELD	GROUP	SUB-GROUP	Modified betatron Equilibrium studies		
			Self-field effects Adiabatic behavior		
			(Continues)		
19 ABSTRACT (Continue on reverse if necessary and identify by block number) An analytic and numerical scheme is developed to follow the adiabatic evolution of a beam with non-zero transverse pressure in a modified betatron. These calculations are made using improvements to previous zero pressure models in regimes where, as before, the poloidal inertia is ignored. The evolution of the beam is determined as a series of time independent equilibria with pressure appearing in our fluid approach as a gradient in the fluid equations of motion. The evolution of the pressure during adiabatic acceleration is determined by kinetic theory. The series of equilibria are then characterized by the constant number of particles within a drift ( $P_\theta$ ) surface, the conserved toroidal flux inside a $P_\theta$ surface, and the self-consistently evaluated pressure distribution (from magnetic moment conservation.) As in the case of zero pressure, it is found that the beam makes a transition from diamagnetic to paramagnetic orbits when it reaches a certain energy, and that the transition manifests itself by a change in the topology of the $P_\theta$ surfaces during acceleration. As compared to our zero pressure results, it is found that the poloidal drift of the beam is significantly faster, so that (Continues)					
20 DISTRIBUTION/AVAILABILITY OF ABSTRACT <input checked="" type="checkbox"/> UNCLASSIFIED/UNLIMITED <input type="checkbox"/> SAME AS RPT <input type="checkbox"/> DTIC USERS			21 ABSTRACT SECURITY CLASSIFICATION <b>UNCLASSIFIED</b>		
22a NAME OF RESPONSIBLE INDIVIDUAL <b>W. M. Manheimer</b>			22b TELEPHONE (Include Area Code) <b>(202) 767-2765</b>		22c OFFICE SYMBOL <b>Code 4791</b>

16. SUPPLEMENTARY NOTATION (Continued)

This work was supported by the Office of Naval Research.

18. SUBJECT TERMS (Continued)

Acceleration  
Transverse pressure effects  
Kinetic theory

19. ABSTRACT (Continued)

→ measurement of this rotation frequency is a possible diagnostic for pressure. Despite the faster drift, however, the paramagnetic transition occurs at about the same energy in both cases. Finally it is observed that the higher poloidal drift frequency associated with this pressure forces the beam toward the Brillouin limit much sooner than in the cold beam case, and that contrary to simple estimates, the pressure increases rather than decreases during acceleration due to a coupling between toroidal and poloidal motion.

## CONTENTS

I. INTRODUCTION .....	1
II. FLUID EQUATIONS AND BETATRON ORDERING .....	3
III. INCORPORATION OF FORMALISM INTO NUMERICAL CODE ....	12
IV. RESULTS .....	16
V. CONCLUSIONS .....	21
ACKNOWLEDGMENT .....	21
REFERENCES .....	28
APPENDIX A: CONSERVATION OF MAGNETIC MOMENT .....	29

**DTIC**  
**ELECTE**  
**DEC 18 1984**  
**B**



Accession For	
NTIS GRA&I	<input checked="" type="checkbox"/>
DTIC TAB	<input type="checkbox"/>
Unannounced	<input type="checkbox"/>
Justification	
By	
Distribution/	
Availability Codes	
Avail and/or	
Dist	Special
A-1	

# ACCELERATION OF AN ELECTRON RING IN A MODIFIED BETATRON WITH TRANSVERSE PRESSURE

## I. Introduction

Interest in the modified betatron derives in part from its promise as a high current accelerator.<sup>1-4</sup> It is designed to overcome the current limitations in a conventional betatron, where the defocusing self-field forces (which scale like  $E/\gamma^2$ , where  $E$  is the self-electric field, and,  $\gamma$  is the relativistic factor) must be less than the focusing forces from the external magnetic field index  $\eta$  ( $0 < \eta < 1$ ). The conventional betatron then has two viable injection regimes - one where the injected energy is low and the current (or density) is low, and the other, where the current (or density) is high and the injected energy is high. The inclusion of an external toroidal field,  $B_\theta$ , in the modified betatron allows injection and trapping at lower energy and high current (1-10 kA). Other theoretical studies of the behavior of this accelerator have either used particle simulations to determine the self-consistent motion,<sup>5,6</sup> or have assumed a given density and current profile and calculated the motion of test particles in fixed fields.<sup>2,3,5,7</sup> The drawback of particle simulations is the large computational cost, particularly because the time scales of acceleration and self-flux diffusion are on the order of  $10^{-4} - 10^{-3}$  sec while the time scale of one particle cyclotron orbit is on the order of  $10^{-10}$  sec. The analytic technique is limited because of the assumed charge and current profile.

In our previous work,<sup>8-10</sup> a theoretical technique is developed to extend the methods mentioned above and to analyze both the self-consistent equilibrium in the modified betatron and the evolution of this equilibrium as external parameters are varied slowly compared to a drift period. These

Manuscript approved August 2, 1984.

calculations assume a cold (zero pressure) beam. In this paper, we expand our theoretical technique and analyze the evolution of equilibria in the modified betatron with transverse pressure.

An investigation is also made to determine if the presence of pressure causes any qualitative changes in behavior which can be measured easily in the experiment; such effects may indicate a useful diagnostic measurement of beam pressure. The effect of random transverse motion appears as a pressure gradient term in the force balance equation in our formalism in a limit that is applicable to current designs for modified betatrons.

As will be shown in the section on our new formalism, we find that many of our earlier results still hold to first order, namely that the fluid canonical angular momentum,  $P_\theta$ , characterizes the equilibria (because many important fluid quantities are functions of  $P_\theta$ , and because surfaces of constant  $P_\theta$  are drift surfaces of single electrons). The pressure  $\Pi$  manifests itself as an additional defocusing force on the beam (with force density  $\sim 2\Pi/a$ ), tending to increase its minor radius  $a$ . The pressure also produces an outward "hoop force" (with force density  $\sim \Pi/R$ ), tending to increase the major radius  $R$  of the beam. These two effects can be seen in our results by: a) an increase in the poloidal  $F_p \times B_t$  drift on the beam (where  $F_p$  represents the total poloidal defocusing force, and  $B_t$  the toroidal magnetic field), and b) a slight increase in the vertical field  $B_z$  necessary to hold the beam at its equilibrium major radius  $R$ .

We have performed two different classes of calculations. The first class involves a series of separate equilibria with similar beam energies but various levels of pressure. The other class involves the calculation of a series of adiabatically coupled equilibria during acceleration. These will be discussed in Section IV.



In Section II our new fluid model, including pressure, is presented. This is followed in Section III with a description of how the new model is incorporated into the numerical code, as well as a qualitative discussion of the effects of pressure on the system. Next, we discuss our results in Section IV and summarize in Section V.

## II. Fluid Equations and Betatron Ordering

In this section we derive fluid equations for a warm relativistic electron beam in a modified betatron. We derive an ordering scheme for diamagnetic equilibria which indicates the conditions under which the transverse thermal spread of the beam can be described by a scalar pressure, and the conditions under which this pressure can be assumed to be constant on the fluid  $P_0$  surfaces.

The first moment of the relativistic Vlasov equation for  $f(\underline{x}, p, t)$  is

$$\frac{\partial}{\partial t} (n \langle p \rangle) + \nabla \cdot \int f \underline{v} p d^3 p = n q \left( \underline{E} + \frac{1}{c} \langle \underline{v} \rangle \times \underline{B} \right), \quad (1)$$

which can, with the aid of the continuity equation  $\partial n / \partial t + \nabla \cdot n \langle \underline{v} \rangle = 0$ , be written in the form

$$n \langle \underline{v} \rangle \cdot \nabla \bar{p} = n q \left( \underline{E} + \frac{1}{c} \langle \underline{v} \rangle \times \underline{B} \right) - \nabla \cdot \bar{\Pi}, \quad (2)$$

for equilibria ( $\partial / \partial t = 0$ ), where  $p = \gamma m v$ ,  $n = \int f d^3 p$ ,  $n \langle \underline{v} \rangle = \int f \underline{v} d^3 p$ ,  $n \langle p \rangle = \int f p d^3 p$ ,

$$\bar{p} = \frac{\int d^3 p f p / \gamma}{\int d^3 p f / \gamma}, \quad (3a)$$

$$= \frac{m \langle v \rangle}{\langle 1/\gamma \rangle}, \quad (3b)$$

and

$$\Pi_{ij} = \int d^3 p \frac{f}{\gamma m} (p_i - \bar{p}_i) (p_j - \bar{p}_j). \quad (4)$$

A manifestly covariant formulation of the fluid equations has recently been described by Newcomb.<sup>11</sup>

The class of equilibria we wish to describe have distribution functions of the form

$$f(H, P_\theta, \mu) = W(P_\theta, \mu) \delta[H - E(P_\theta)], \quad (5)$$

where  $H$  is the particle energy  $\gamma mc^2 + q\phi$ ,  $P_\theta = \gamma m r v_\theta + q\psi/c$  is the canonical angular momentum ( $\psi = rA_\theta$ ), and

$$\mu(r, p) = \frac{(p_\perp - \bar{p}_\perp)^2}{2B_\theta(r, z)}, \quad (6)$$

is the first adiabatic invariant. Here,  $(r, \theta, z)$  is a cylindrical coordinate system with  $z$  the vertical direction and  $\theta$  referring to the toroidal symmetry direction. Also,  $\perp$  refers to components perpendicular to the toroidal magnetic field  $B_\theta \hat{\theta}$ . The conditions under which  $\mu$  is invariant are discussed in Appendix A. This distribution function has a distribution of magnetic moment  $\mu$  and contains the cold beam case of Refs. 8 and 9 as a special case  $W(P_\theta, \mu) = W_0(P_\theta) \delta(\mu)$ .

In general, a distribution such as (5) cannot be required to have only transverse thermal spread, in spite of the delta function in energy, because

the distribution of  $\mu$ . That is, no element of the stress tensor  $\Pi$  given in Eq. (4) is exactly zero unless the distribution is cold. Nevertheless, there is an ordering scheme appropriate to the modified betatron in which  $\Pi$  is isotropic in the poloidal plane  $(r, z)$ . Defining  $\omega_p$  to be the plasma frequency and  $\omega_c$  to be the (nonrelativistic) cyclotron frequency in the toroidal field,  $B_v$  the externally imposed vertical field, and  $\omega_{cv} = eB_v/mc$ , we take

$$\frac{\omega_p^2}{\omega_c^2} = O(1), \quad (7a)$$

$$\frac{a}{R} = O(\epsilon^2), \quad (7b)$$

$$\gamma = O(\epsilon^{-1-\delta}), \quad (7c)$$

$$\frac{B_v}{B_\theta} = O(\epsilon^{1-\delta}), \quad (7d)$$

$$\frac{\gamma c}{\omega_{cv} R} = O(1), \quad (7e)$$

$$\frac{\rho}{a} = O(\epsilon^{2/3}). \quad (7f)$$

Here,  $\rho$  is the electron gyroradius in the toroidal field,  $a$  is the minor radius of the beam and  $R$  the major radius. Since this ordering must describe the beam from injection ( $\gamma \sim 4$ ) up to the diamagnetic-paramagnetic transition ( $\gamma \gtrsim 15$ ), and since the ratio of  $eE/\gamma^2$  to focusing forces scales as  $1/\gamma^3$ , the extra parameter  $\delta$  is required for the ordering to be valid throughout the acceleration. For parameters relevant to the NRL modified betatron,  $\epsilon \sim 1/10$ ; also,  $\delta \sim -1/3$  corresponds to injection and  $\delta \sim 1/3$  corresponds to transition.

Note that the scalings with  $\delta$  in Eq. (7) reflect the invariants of motion during acceleration or any adiabatic evolution of the beam. In particular,  $\omega_p^2/\omega_c^2$  is independent of time (i.e. of  $\delta$ ) because conservation of the total toroidal flux  $\Phi$  through the beam<sup>8,9</sup> implies that the density remains approximately constant, and the acceleration scheme we are concerned with does not involve changing the external toroidal magnetic field. (The self magnetic field is smaller in this ordering.) Similarly, relation Eq. (7e) represents the fact that  $\gamma$  is proportional to  $B_\theta$  during acceleration, due to  $P_\theta$  conservation. Finally, since  $\mu$  is the flux through the gyro-orbit, relation Eq. (7f) follows from  $\rho/a \sim (\mu/\Phi)^{1/2}$ . Also, Eq. (7f) guarantees that the electron velocity about the guiding center  $\rho\omega_c/\gamma$  is of the same order as the drift velocity  $cE/\gamma^2 B$  at injection, a plausible assumption for most injection schemes. In fact, for this ordering we find that the drift and gyration velocities obey  $v_d/c \sim \epsilon^{2+2\delta}$  and  $v_g/c \sim \epsilon^{\delta+5/3}$ . With this ordering, we find that the forces  $eE/\gamma^2$ ,  $e v_\perp B_\theta/c$ , the external focusing forces, and the pressure gradient are in relation

$$\epsilon^{1+3\delta}; \epsilon^{1+3\delta}; \epsilon^2; \epsilon^{2\delta+4/3}. \quad (8)$$

We see that the first two forces dominate at injection ( $\delta = -1/3$ ), whereas all four are of the same order at transition ( $\delta = 1/3$ ). Note that for intermediate times,  $-1/3 < \delta < 1/3$ , the pressure gradient dominates focusing forces. Also note that  $q\phi/\gamma mc^2 \sim v/\gamma \sim 1/\gamma \sim \epsilon^{1+\delta}$ .

Using this ordering we first estimate the distribution of  $\gamma$  which is due to the distribution of  $\mu$  shown in Eq. (5). Assuming the energy  $E(P_\theta) = E_0 + \Omega(P_\theta - P_{\theta 0})$  as in Ref. 8,  $H = E(P_\theta)$  from Eq. (5) and the definition of  $\gamma$  give

$$\gamma mc^2 - \gamma m r \Omega v_\theta = H_0(r, z) \equiv E_0 - \Omega p_{\theta 0} + q \Omega \Psi / c - q \phi, \quad (9a)$$

$$\gamma^2 = 1 + p_\theta^2 / m^2 c^2 + (p_{ld} + p_{lg})^2 / m^2 c^2, \quad (9b)$$

where  $p_\theta = \gamma m v_\theta$ ,  $p_{ld}$  is the momentum associated with the guiding center drift, and  $p_{lg}$  is the momentum associated with gyration about the guiding center. From Eq. (7) we find  $p_{ld}^2 \sim \epsilon^{2+2\delta}$ ,  $p_{lg}^2 \sim \epsilon^{4/3}$ , the latter constant since it is essentially magnetic moment. Putting Eqs. (9) in dimensionless form by defining  $q_\theta = p_\theta / mc$ ,  $q_\perp = p_\perp / mc$ ,  $K = H_0(r, z) / mc^2$ , and  $\omega = r \Omega / c$  and combining, we find

$$1 + q_\theta^2 + q_\perp^2 = (K + \omega q_\theta)^2. \quad (10)$$

Expanding for  $q_\perp^2 \ll 1$ ,  $K \gg 1$  [from Eq. (7), these quantities scale as  $\epsilon^{4/3}$  and  $\epsilon^{-1-\delta}$ , respectively], i.e. treating  $1 + q_\perp^2$  as a perturbation in Eq. (10), we find

$$q_{\theta 0} = \frac{K}{1 - \omega}, \quad (11a)$$

$$\delta q_\theta = - \frac{1 + q_\perp^2}{2K}, \quad (11b)$$

$$\gamma_0 = \frac{K}{1 - \omega}, \quad (11c)$$

$$\delta \gamma = - \frac{\omega(1 + q_\perp^2)}{2K}. \quad (11d)$$

Therefore, the thermal contribution to  $\delta q_\theta$  and  $\delta \gamma$ ,  $\delta q_{\theta t} = -q_{lg}^2 / 2K$  and

$\delta\gamma_t = -\omega q_{lg}^2/2K$ , satisfy

$$\frac{\delta q_{\theta t}}{q_{\theta 0}} \sim \frac{\delta\gamma_t}{\gamma_0} \sim \epsilon^{10/3} + 2\delta. \quad (12)$$

Also

$$\frac{\delta v_{\theta}}{c} = \frac{\delta q_{\theta}}{\gamma_0} - \frac{q_{\theta 0} \delta\gamma}{\gamma_0^2} = -\frac{(1-\omega)^2(1+q_1^2)}{2K^2}, \quad (13)$$

the thermal contribution to which has

$$\frac{\delta v_{\theta t}}{c} \sim \frac{q_{lg}^2}{K^2} \sim \epsilon^{10/3} + 2\delta. \quad (14)$$

Using  $q_{ld}^2 \sim \epsilon^2 + 2\delta$ ,  $q_{lg}^2 \sim \epsilon^{4/3}$ , we find that the drift contributions to  $\delta q_{\theta}$ ,  $\delta\gamma$  and  $\delta v_{\theta}$  are smaller than the thermal contributions for  $\delta > -1/3$ . The issue of conservation of  $\mu$  in this ordering is addressed in Appendix A.

We now use the relations Eqs. (11)-(14) to evaluate the stress tensor  $\Pi$  of Eq. (4) for equilibrium distribution functions of the form Eq. (5). First, noting  $d^3p = (B_{\theta}/r) d\mu d\chi dP_{\theta}$ , where  $\chi = \tan^{-1}[(p_z - \bar{p}_z)/(p_r - \bar{p}_r)]$  is the gyrophase, we find that the density is given by

$$n = \frac{B_{\theta}}{r} \int d\mu d\chi \int \frac{dP_{\theta} W(P_{\theta}, \mu) \delta[P_{\theta} - \tilde{P}_{\theta}(r, z, p_{\perp}^2)]}{v_{\theta}/r - \Omega(P_{\theta})}, \quad (15)$$

where  $P_{\theta} = \tilde{P}_{\theta}(r, z, p_{\perp}^2)$  is the solution of  $H = E(P_{\theta})$ , found in Eqs. (9) - (11) for the special case  $\Omega = dE/dP_{\theta} = \text{const.}$  For this case, we find

$$\tilde{p}_\theta(r, z, p_\perp^2) = p_\theta^{(0)}(r, z) + mcr\delta q_\theta, \quad (16)$$

where  $p_\theta^{(0)}$  neglects the drift and thermal corrections in Eq. (9). From the above ordering, the thermal and drift contributions to  $\tilde{p}_\theta$  and  $v_\theta$  are negligible and we find

$$n = \frac{2\pi B_\theta}{v_{\theta 0} - r\Omega} \int_0^\infty d\mu W[p_\theta^{(0)}(r, z), \mu]. \quad (17)$$

Also, using this ordering we find that  $\bar{p} = \langle p \rangle = \gamma_0 m \langle v \rangle$  in Eq. (12) and that the two diagonal poloidal components of the stress tensor are

$$\begin{aligned} \Pi_{rr} &= \Pi_{zz} \\ &= \frac{2\pi B_\theta^2}{\gamma_0 m (v_{\theta 0} - r\Omega)} \int_0^\infty \mu d\mu W[p_\theta^{(0)}(r, z), \mu], \end{aligned} \quad (18)$$

while the off diagonal terms are

$$\begin{aligned} \Pi_{rz} &= \Pi_{zr} \\ &= \frac{2B_\theta^2}{m} \int d\mu d\chi \sin \chi \cos \chi \int \frac{dp_\theta}{\gamma(v_\theta - r\Omega)} W(p_\theta, \mu) \\ &\quad \times \delta[p_\theta - \tilde{p}_\theta(r, z, p_\perp^2)]. \end{aligned} \quad (19)$$

If we neglect the thermal and drift corrections to  $\tilde{p}_\theta$ ,  $\gamma$ , and  $v_\theta$ , these terms vanish by the integration over the gyrophase  $\chi$ . By similar considerations we find  $\Pi_{\theta r} = \Pi_{\theta z} = \Pi_{r\theta} = \Pi_{z\theta} = \Pi_{\theta\theta} = 0$ . Thus,  $\nabla \cdot \Pi = \nabla \Pi(r, z)$ , with  $\Pi = \Pi_{rr} = \Pi_{zz}$ .

Using these conclusions, we find that the toroidal component of the equation of motion, Eq. (2)

$$n\mathbf{v} \cdot \nabla \bar{p}_\theta + \frac{nv_\theta}{r} \bar{p}_r = -\frac{nq}{rc} \mathbf{v} \cdot \nabla \psi - \frac{\partial}{\partial r} \Pi_{r\theta} - \frac{\partial}{\partial z} \Pi_{z\theta} - \frac{2}{r} \Pi_{r\theta}, \quad (20)$$

gives

$$\mathbf{v}_p \cdot \nabla (\gamma_0 m r v_{\theta 0} + q\psi/c) = 0. \quad (21)$$

Since the poloidal velocity  $\mathbf{v}_p$  is  $\mathbf{j}_p/ne = (c/4\pi ne)\nabla g \times \nabla \theta$  ( $\mathbf{B} = \nabla \psi \times \nabla \theta + g\nabla \theta$ ), and since the quantity in parentheses in Eq. (21) is  $p_\theta^{(0)}$ , we find, as in the cold fluid case, Ref. 9

$$g = g(p_\theta^{(0)}). \quad (22)$$

The poloidal components of the equation of motion, neglecting poloidal centrifugal force, are

$$\begin{aligned} 0 &= \frac{\gamma_0 m v_{\theta 0}^2}{r} \nabla r - q \nabla \phi + \frac{qv_\theta}{rc} \nabla \psi - \frac{gg'(p_\theta^{(0)})}{4\pi nr^2} \nabla p_\theta^{(0)} - \frac{\nabla \Pi}{n} \\ &= \frac{v_{\theta 0}}{r} \nabla p_\theta^{(0)} - m v_{\theta 0} \nabla (v_{\theta 0} \gamma_0) - q \nabla \phi - \frac{gg'}{4\pi nr^2} \nabla p_\theta^{(0)} - \frac{\nabla \Pi}{n}. \end{aligned} \quad (23)$$

To lowest order in  $\epsilon$ ,  $\Pi$ , given by Eq. (18) is a function of  $p_\theta^{(0)}$ . Specifically, the relative variation of  $B_\theta^2 = g(p_\theta)^2/r^2$  scales as  $\delta r/r_0 \sim \epsilon^2$ , and the relative variation of  $\gamma_0$  is  $e\Delta\phi/\gamma mc^2$ , where  $\Delta\phi$  is the variation of  $\phi$  along a  $p_\theta$  surface. For highly elongated drift surfaces, as can occur near transition,<sup>8,9</sup> the quantity scales as  $\gamma^{-1} \sim \epsilon^{1+\delta}$  [See Appendix A]. For circular flux surfaces, the relative variation of  $\phi$  along a  $p_\theta$  surface (due to



the toroidally generated displacement between these surfaces) is of order  $a/R \sim \epsilon^2$ , so  $\delta\gamma/\gamma$  scales as  $\epsilon^{3+\delta}$ . Finally, the denominator  $v_{\theta 0} - r\Omega$  scales as  $\delta r/r_0 \sim \epsilon^2$  as long as the two terms which make up the denominator do not nearly cancel. Thus the relative change in pressure along a  $P_\theta$  surface is at worst  $\epsilon^{1+\delta}$ . In fact, away from transition, the flux surfaces are nearly always circular so the relative pressure variation is actually much less. Since the pressure itself is not a dominant effect except near transition (see Eq. (8)), the variation of  $\Pi$  along a  $P_\theta$  surface is negligible. Thus  $\Pi(r, z) = \Pi(P_\theta)$ . Using these relations, which imply  $v_{\theta 0} \nabla(v_{\theta 0} \gamma_0) \simeq c^2 \nabla \gamma_0$  and  $\nabla \Pi = \Pi'(P_\theta^{(0)}) \nabla P_\theta^{(0)}$ , we find (dropping the 0 superscripts)

$$\left(\frac{v_\theta}{r} - \frac{dE}{dP_\theta}\right) \nabla P_\theta = \left(\frac{gg'(P_\theta)}{4\pi r^2} + \frac{\Pi'(P_\theta)}{n}\right) \nabla P_\theta. \quad (24)$$

We can use this equation to solve for the density, obtaining

$$n = \frac{r}{v_\theta - r\Omega(P_\theta)} \left[ \frac{gg'(P_\theta)}{4\pi r^2} + \Pi'(P_\theta) \right]. \quad (25)$$

Note that this reduces to the non-relativistic MHD result

$j_\theta = cr[gg'(\psi)/4\pi r^2 + \Pi'(\psi)]$ , obtained from  $\mathbf{j} \times \mathbf{B} = c\nabla\Pi$ , when inertia and electric field vanish ( $P_\theta \rightarrow q\psi/c$ ,  $\Omega \rightarrow 0$ ).

It is worth noting that  $\Pi$  can be specified to be an arbitrary function of  $P_\theta$ . Indeed, using the approximations under which  $\Pi$  is a function of  $P_\theta$  alone we can write

$$\Pi(P_\theta) = Y(P_\theta) \int_0^\infty u du W(P_\theta, u), \quad (26)$$

where  $Y(P_\theta)$  is a drift surface average of  $2\pi B_\theta^2 / [\gamma_0 m (v_{\theta 0} - r\Omega)]$ . We can find a

large class of functions  $W(P_\theta, \mu)$  that produce  $\Pi(P_\theta)$ , for example

$$W(P_\theta, \mu) = W_0(P_\theta) \delta[\mu - \bar{\mu}(P_\theta)], \quad (27)$$

with the condition  $W_0(P_\theta) \bar{\mu}(P_\theta) = \Pi(P_\theta)/Y(P_\theta)$ .

### III. Incorporation of Formalism into Numerical Code

In this section we will discuss the incorporation of our new pressure formalism into the original computer code. The calculation of a single equilibrium (or the first in a series of equilibria adiabatically connected) proceeds as in our previous work,<sup>8-10</sup> except that the density is calculated using Eq. (25). For convenience we model the initial density, pressure gradient, and  $K(P_\theta) = gg'(P_\theta)$  as linear functions of  $P_\theta$ ;

$$K(P_\theta) = K_0(P_{\theta c} - P_\theta)/(P_{\theta c} - P_{\theta o}), \quad (28)$$

and

$$\Pi'(P_\theta) = -2\Pi_0(P_{\theta c} - P_\theta)/(P_{\theta c} - P_{\theta o})^2, \quad (29)$$

where  $P_{\theta c}$  is the value of  $P_\theta$  at the edge of the beam, and  $P_{\theta o}$  is the (conserved) minimum value of  $P_\theta$  at the center of the beam. Equation (29) gives a quadratic pressure profile in  $P_\theta$ ,

$$\Pi(P_\theta) = \Pi_0 \frac{(P_{\theta c} - P_\theta)^2}{(P_{\theta c} - P_{\theta o})^2}. \quad (30)$$

Since the maximum density  $n(P_{\theta o})$  and maximum pressure  $\Pi_0$  are determined from

the input parameters (of injected current and peak pressure), the constant  $K_0$  can be determined from Eqs. (25), (28)-(29). (Note that as in our previous work, we choose  $\Omega(P_\theta) = \text{constant}$ .)

By integrating Eq. (25) over drift surfaces, we obtain

$$\frac{dN}{dP_\theta} = \frac{1}{2} g g' \int \frac{dl}{|v P_\theta|} \frac{1}{(v_\theta - r\Omega)} + 2\pi \Pi'(P_\theta) \int \frac{dl}{|v P_\theta|} \frac{r^2}{(v_\theta - r\Omega)}, \quad (31)$$

where the quantity  $(dN/dP_\theta)\delta P_\theta$  is the (conserved) number of particles between drift surfaces labeled by  $P_\theta$  and  $P_\theta + \delta P_\theta$ . In our iterative solution of the equilibrium equations defining the system we conserve the initial values of  $dN/dP_\theta$ , the beam's equilibrium major radius  $R$  (location of  $v P_\theta = 0$ ), the minimum  $P_{\theta 0}$ , and the toroidal flux in the beam  $\Phi_t$ . During the adiabatic evolution of these equilibria, the change in pressure must be determined as external parameters change adiabatically.

We begin with Eq. (18), defining the pressure in our ordering scheme

$$\Pi = \Pi_{rr} = \frac{2\pi B_\theta^2}{\gamma_0(t)m(v_{\theta 0}(t) - r\Omega(t))} \int_0^\infty \mu d\mu W[P_\theta^{(0)}(r, z), \mu].$$

To lowest order,  $\Pi = \Pi(P_\theta)$ , but since  $B_\theta$ , and  $(v_{\theta 0} - r\Omega)$  vary along a  $P_\theta$  surface, let us redefine the pressure as

$$\Pi(P_\theta) = \left\langle \frac{2\pi B_\theta^2}{\gamma_0 m(v_{\theta 0} - r\Omega)} \right\rangle_{P_\theta} \cdot \int_0^\infty W(P_\theta, \mu) \mu d\mu, \quad (32)$$

where  $\langle \rangle_{P_\theta}$  is an average over a  $P_\theta$  surface.

The integral in Eq. (32) does not change in time ( $\mu$ , and  $P_\theta$  are constants of the motion), while the term inside the brackets changes as  $\gamma_0$ ,  $\beta$ ,  $\Omega$ , and the shape of  $P_\theta$  surfaces change in time. Using Eq. (32) we can determine the

evolution of  $\Gamma(P_\theta, t)$  in time from

$$\frac{\Pi(P_\theta, t)}{\Pi(P_\theta, 0)} = \frac{g^2(P_\theta, t)}{g^2(P_\theta, 0)} \frac{\langle \frac{1}{\gamma_0(t) r^2 (\beta_{\theta 0}(t) - \omega(t))} \rangle P_\theta(t)}{\langle \frac{1}{\gamma_0(0) r^2 (\beta_{\theta 0}(0) - \omega(0))} \rangle P_\theta(0)}, \quad (33)$$

where  $g = rB_\theta$ , and  $\omega = r\Omega/c$ . During acceleration,  $gg'(P_\theta)$  is determined from Eq. (31),  $g$  is found by integration of  $gg'$ , and Eq. (33) gives  $\Gamma(P_\theta, t)$ . Since  $gg'$  itself depends on  $\Gamma(P_\theta)$  in Eq. (31), the cycle must be iterated until it converges.

An interesting consequence of Eq. (33) is that pressure actually increases during acceleration. A simple theory for an infinitely long cylindrical beam would specify  $p_\perp$  as a constant of motion during acceleration by a longitudinal electric field. Therefore it would predict  $\Pi \sim p_\perp v_\perp \sim p_\perp^2/\gamma \sim \mu/\gamma$ , or  $\Pi \sim 1/\gamma$ . It can be seen from Eq. (33) however, that  $p$  actually scales as

$$\Pi \sim \langle \frac{1}{\gamma(t) (\beta_\theta(t) - \omega(t))} \rangle P_\theta. \quad (34)$$

During acceleration  $\gamma$  increases, but  $(\beta_\theta(t) - \omega(t))$  decreases faster, with the net effect that the pressure increases. This increase in pressure arises from the fact that the parallel and perpendicular parts of the momentum are coupled by the poloidal field and toroidal geometry. The tendency of  $\beta_\theta - \omega$  to decrease, i.e. for  $\Omega \equiv dE/dP_\theta$  to increase, is due to toroidal flux invariance as discussed in Ref. 9. It will be seen in our acceleration results that the increasing pressure drives the poloidal drift of the beam toward the Brillouin limit as the beam accelerates. A brief explanation of how the pressure affects this drift may be useful.

Let  $\rho$  denote distance from beam center. Then assuming a quadratic dependence of  $P_\theta$  on  $\rho$  near the reference orbit we can write

$$P_\theta = P_{\theta 0} + (P_{\theta c} - P_{\theta 0})\rho^2/a^2, \quad (35)$$

where  $a$  is the beam radius.

Substituting Eq. (35) into Eq. (30) gives

$$\Pi(\rho) = \Pi_0(1 - \rho^2/a^2)^2. \quad (36)$$

The pressure gradient plays a defocusing role in poloidal force balance as can be seen by writing the poloidal fluid equation of motion near the reference orbit

$$m\gamma \frac{v^2}{\rho} + \frac{qE}{\gamma^2} + \frac{qv}{c} B_\theta + \frac{4\Pi_0\rho}{na^2} = 0, \quad (37)$$

where  $qE/\gamma^2$  represents the sum of the self electric and self magnetic  $(v_\theta \times B_{\text{self}})$  forces<sup>8,9</sup> and  $v$  is the poloidal velocity. Equation (37) can be rewritten in terms of the poloidal rotational frequency  $\Omega_D = v/\rho$  as

$$2\gamma^3\Omega_D^2 + \omega_p^2 + \frac{8\gamma^2\Pi_0}{na^2m} - 2\gamma^2\omega_c\Omega_D = 0, \quad (38)$$

where  $\omega_p$  is the plasma frequency, and  $\omega_c$  is the (non-relativistic) cyclotron frequency in the toroidal field. From the solution of Eq. (38)

$$\Omega_D = \frac{\omega_c}{2\gamma} \pm \frac{1}{2\gamma} \sqrt{\omega_c^2 - \frac{2}{\gamma}(\omega_p^2 + 8\Pi_0\gamma^2/na^2m)}, \quad (39)$$

it can be seen that the maximum (real) value of  $\Omega_D$  is still  $\Omega_D = \omega_c/2\gamma$ , the Larmor frequency at Brillouin flow, but that the pressure serves to increase  $\Omega_D$  in the slow mode, effectively adding diamagnetic drift to the  $E \times B/\gamma^2$  drift.

#### IV. Results

##### A. Decoupled Pressure Equilibria

In this first set of calculations, we hold certain macroscopic quantities fixed and find beam equilibria for different values of pressure. At each level of pressure, the beam energy at its center, the total number of particles, the peak density, external toroidal field, and the toroidal flux in the beam are the same, but the calculations are not adiabatically coupled.

Two sets of calculations are discussed here. In one case a 1 kA beam with  $\gamma = 4$ , minor radius  $a = 2$  cm, and major radius  $R = 100$  cm is injected into a toroidal conducting chamber with circular cross section of minor radius 12.5 cm, and major radius 100 cm (see Fig. 1). The applied vertical field  $B_z$  is initially set equal to 71.46 gauss but adjusts itself slightly to maintain the beam at its major radius. We set the field index  $\eta = 0.5$  at beam center. The applied toroidal field  $B_\theta$  is held at 2000 gauss. We varied the pressure from 80 to 320 dynes/cm<sup>2</sup>. As a point of reference we estimate a pressure which corresponds to the Lawson-Penner emittance  $\epsilon_{L-P} = 0.3\sqrt{I}$  (kA) rad-cm. Writing pressure in terms of the transverse velocity,  $\Pi = \gamma m n v_\perp^2$ , and relating it to the normalized "emittance"  $\epsilon_n = \gamma \beta a v_\perp / v_0$ , ( $v_0$  = beam velocity,  $a$  = beam radius) we get  $\Pi = n m v_0^2 \epsilon_n^2 / \gamma \beta^2 a^2$ . Setting  $\epsilon_n = \epsilon_{L-P}$  gives  $\Pi_{L-P} = 187$  dynes/cm<sup>2</sup> for the 1 kA beam. In an unmagnetized system, this emittance corresponds roughly to random transverse energy. In a magnetized system with

an immersed cathode, this random transverse energy is manifested as finite Larmor radius (non-zero  $\mu$ ) for the electrons.

The only quantity which responded significantly to this pressure variation is the poloidal drift  $\bar{\Omega}_D$  averaged across the beam. This term is plotted in Fig. 2(a) as a function of pressure. In Fig. 2(b) we show the average Larmor radius associated with the pressure (this quantity is derived from the simple relations  $\Pi = \gamma m n v_\perp^2$  and  $r_b = \gamma m c v_\perp / e B_\theta$ ). Note that the poloidal drift of the beam is calculated from  $\nabla \times \underline{B} = 4\pi \underline{J}/c$ , giving a drift velocity  $\hat{v}_d = c(\nabla g \times \hat{\theta})/(4\pi n q r)$  in our notation. The drift frequency associated with  $\hat{v}_d$  is averaged across the beam and normalized to the Larmor rotational frequency at the Brillouin limit  $\Omega_B = 4.41 \times 10^9 \text{ sec}^{-1}$ .

Other quantities such as the vertical magnetic field  $B_z$  necessary to maintain R, the toroidal field  $B_\theta$  at beam center the poloidal flux at beam center, and the profiles of the electrostatic potential  $\phi$  and poloidal flux  $\psi$ , changed less than 0.2% over this range of emittances. The vertical field increased to compensate for the increased hoop forces, and the  $B_\theta$  field decreased because of the faster diamagnetic drift.

In our second case, we use a 10 kA beam with the same geometrical features (a, R, etc.). The vertical field is initially 120.1 gauss and the applied toroidal field is set again at 2000 gauss. This time we varied the pressure from  $1. \times 10^3$  to  $9. \times 10^3 \text{ dynes/cm}^2$ , where  $\Pi_{L-P} = 21.5 \times 10^3 \text{ dynes/cm}^2$ . The Larmor frequency in this 10 kA case is  $4.5 \times 10^9 \text{ sec}^{-1}$ ; it is slightly larger than the 1 kA case because of a space charge depression of  $\gamma$ .

As in the previous case, the poloidal drift  $\bar{\Omega}_D$  increases with the pressure. The drift frequency is plotted in Fig. 3(a), with the Larmor radius in Fig 3(b). All of the other diagnostic quantities mentioned above vary less than 0.8%.

The quantity which depends most sensitively on transverse pressure is the poloidal rotation frequency of the electron cloud. This indicates that measuring this rotation frequency could be a very useful diagnostic of transverse pressure. In HIPAC<sup>12</sup> the rotation frequency was measured and used as a diagnostic for total charge. In the modified betatron, because of the cancellation of self electric  $\gamma$  magnetic field, the rotation frequency is much less sensitive to charge and much more sensitive to pressure. Thus if the total charge could be measured in a different way (say by laser scattering), then the rotation frequency could be used as a diagnostic for pressure.

#### B. Adiabatic Acceleration with Pressure

In this next series of calculations, we examine the effect of pressure on beam acceleration in a modified betatron. The evolution of the pressure during acceleration is calculated self-consistently according to the formalism described in Section II. In other respects, however, the techniques used here follow those of Refs. 8-10.

We compare several sets of calculations encompassing a wide range of injection currents (1-10 kA) and pressures (0 - "Lawson-Penner"). As before, we inject a  $\gamma = 4$  beam with minor radius  $a = 2$  cm and major radius  $R = 100$  cm into a toroidal conducting chamber with minor radius 12.5 cm and major radius 100 cm. A variable external vertical  $B_z$  field is used to accelerate the beam and hold it at its equilibrium radius, while an external toroidal  $B_\theta$  field (of 2000 gauss) is used to provide beam equilibrium during the early, diamagnetic stage of acceleration. Our calculations follow the acceleration until the edge of beam comes close to reversing its diamagnetic rotation.

In each case, we choose the initial pressure so that the beam's rotational frequency remains below the Brillouin limit (the Larmor frequency)



throughout the acceleration cycle. This is to ensure that our underlying assumption of small poloidal centrifugal forces remains valid.

In Fig. 4, we plot the rotational frequency  $\bar{\Omega}_D$  of the beam (calculated by averaging  $\Omega_D$  across the beam) during acceleration for various injection currents. The beams were injected with  $I_0 = 1$  kA, 3 kA and 10 kA, and with initial pressures of 100, 800 and 8000 dynes/cm<sup>2</sup> respectively. For reference, the "Lawson-Penner pressure" for each case is 187,  $1.80 \times 10^3$ , and  $21.5 \times 10^3$  dynes/cm<sup>2</sup> respectively. (These do not scale exactly as  $I^2$  because the peak density obtained from the code does not scale exactly as  $I$ .) In addition, the peak pressure as a function of beam energy is plotted in Fig. 5 for these injection currents. The rotational frequencies of Fig. 4 are plotted as ratios of the Brillouin limit frequency  $\Omega_L = eB_0/(2\pi\gamma c)$  which decreases as the beam accelerates, but the trend towards the Brillouin limit is a characteristic of beams with pressure. Zero pressure beams rotate with frequencies that tend away from the Larmor frequency as the beam accelerates (see Fig. 6). The increase in peak pressure with acceleration is responsible for these effects. Higher pressure gradients (near the center of the beam) produce larger defocusing forces and hence a faster drift ( $\vec{F}_p \times \vec{B}_0$ ) in the  $B_0$  field. As discussed in Section III, the increase of pressure with acceleration is an unexpected result with a rather subtle cause (see Eq. (34)).

The Larmor radius of the beam is not calculated independently in our formalism, but from the conservation of magnetic moment  $\mu = \pi r_L^2 B_0$  we conclude that  $r_L$  changes very little during acceleration because the relative change in  $B_0$  due to poloidal beam current is small.

One interesting result we have observed is that the diamagnetic transition appears to occur at about the same energy for beams with pressure

as those without, despite the larger average poloidal drift for "warm" beams. For a 10 kA beam injected at  $\gamma = 4$ , for instance, we find by extrapolation that the edge of the beam undergoes the transition at about  $\gamma = 13.0$  for both the warm [ $\Pi_0(t = 0) = 8 \times 10^3 \text{ dynes/cm}^2$ ] and the cold beam. There are several reasons for this apparent anomaly. First of all, we note that the transition from diamagnetic to paramagnetic rotation is determined in our calculations by following the separatrix of the  $P_\theta$  surfaces as it approaches the beam from the region outside the beam. In this region, the  $P_\theta$  surfaces are also outside the direct influence of the pressure since pressure vanishes outside the beam. Indirectly, the presence of pressure influences the region outside the beam because pressure produces an outward hoop force which increases the vertical field necessary to hold the beam at R, which in turn increases the index focusing forces throughout the system. This effect is very small as noted in our decoupled pressure section. Secondly, note that the effect of pressure within the beam depends on distance  $\rho$  from beam center. As seen in Eq. (36), our pressure has a quartic profile  $\Pi = \Pi_0 (1 - \rho^2/a^2)^2$ . With this profile the pressure gradient is largest inside the beam and drops off to zero near the edge, producing larger diamagnetic drift frequencies at the center of the beam than near the edge.

According to these arguments, and because the defocusing effect of self-electric and self-magnetic fields ( $\sim E/\gamma^2$ ) is essentially the same for beams with and without pressure, we see that the diamagnetic-paramagnetic transition can occur at the beam's edge at roughly the same beam energy. However, the pressure will undoubtedly affect the actual drift reversal of the particles inside the beam, which occurs after transition.

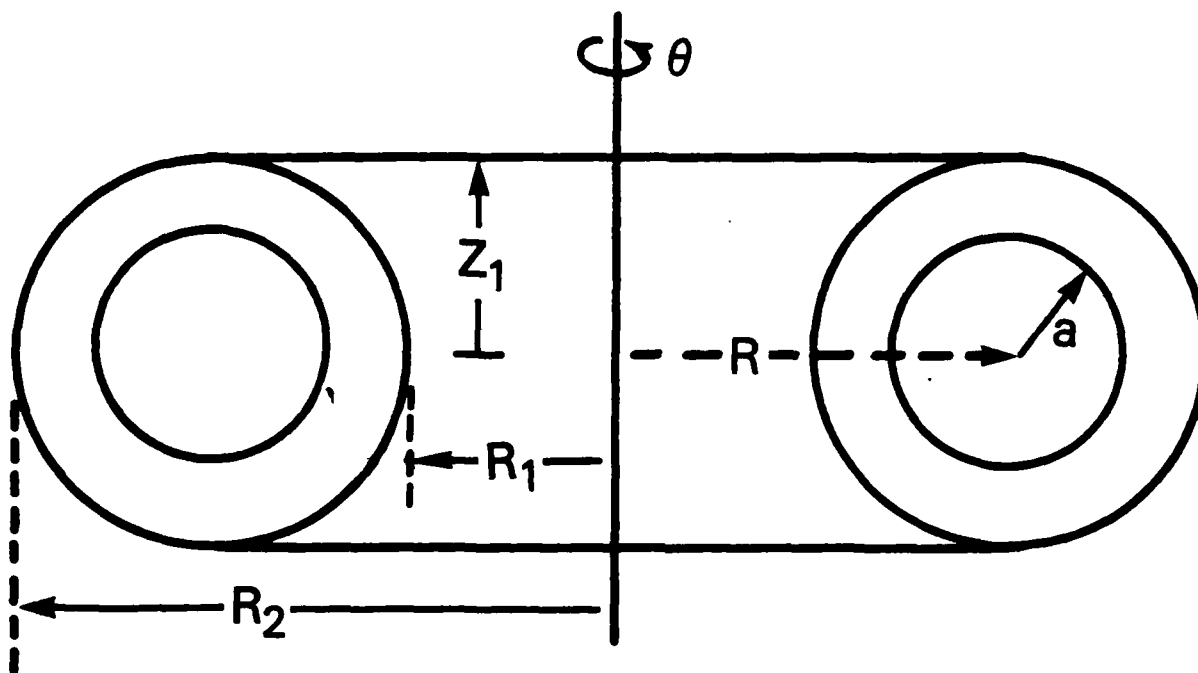
## V. Conclusions

In our analysis of pressure effects on the modified betatron we have assumed that: a) the poloidal drift in the toroidal field is below the Brillouin limit, b) that the parameters affecting the beam change adiabatically, and c) that the parameters of the experiment obey the ordering in Eq. (7). We find that, as expected, the pressure increases the poloidal drift frequency of the beam because of the larger defocusing force. In spite of this increase, however, the diamagnetic to paramagnetic transition begins at about the same energy as a cold beam during acceleration because of the limited scope of the pressure outside the beam. Although our calculations cannot treat the diamagnetic to paramagnetic transition, we speculate that the actual transition process will be much different in the warm beam case. We also find, contrary to simple estimates, that the pressure increases rather than decreases during acceleration.

Finally, we remark that the sensitive dependence of the poloidal drift frequency on the pressure could be used as a diagnostic of transverse pressure by employing the same techniques to measure beam rotation as used in HIPAC.

## Acknowledgment

This work was supported by the Office of Naval Research.



$$\begin{aligned} Z_1 &= 12.5 \text{ cm} \\ R_1 &= 87.5 \text{ cm} \\ R_2 &= 112.5 \text{ cm} \\ R &= 100.0 \text{ cm} \end{aligned}$$

$$\begin{aligned} a &= 2 \text{ cm} \\ E_0 &= 5.584 \times 10^{-6} \text{ ERGS} \\ \gamma_0 &= 4.0 \\ I &= 10.0 \text{ kA} \\ B_\theta &= 2.0 \text{ kGAUSS} \end{aligned}$$

Fig. 1 Schematic of modified betatron with typical parameters.

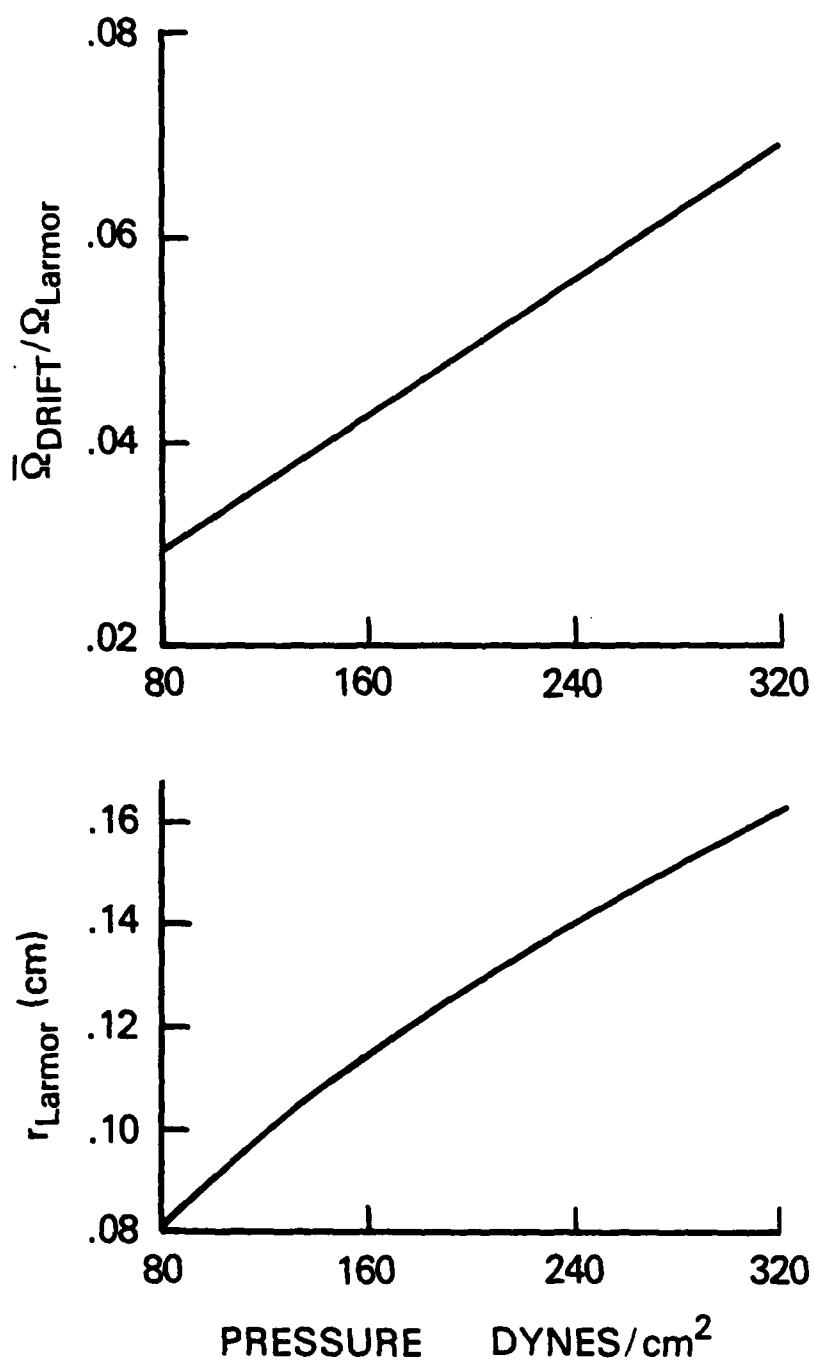


Fig. 2 Poloidal drift and Larmor radius vs. pressure for a 1 kA beam.

$$\Pi_{L-P} = 187 \text{ dynes/cm}^2.$$

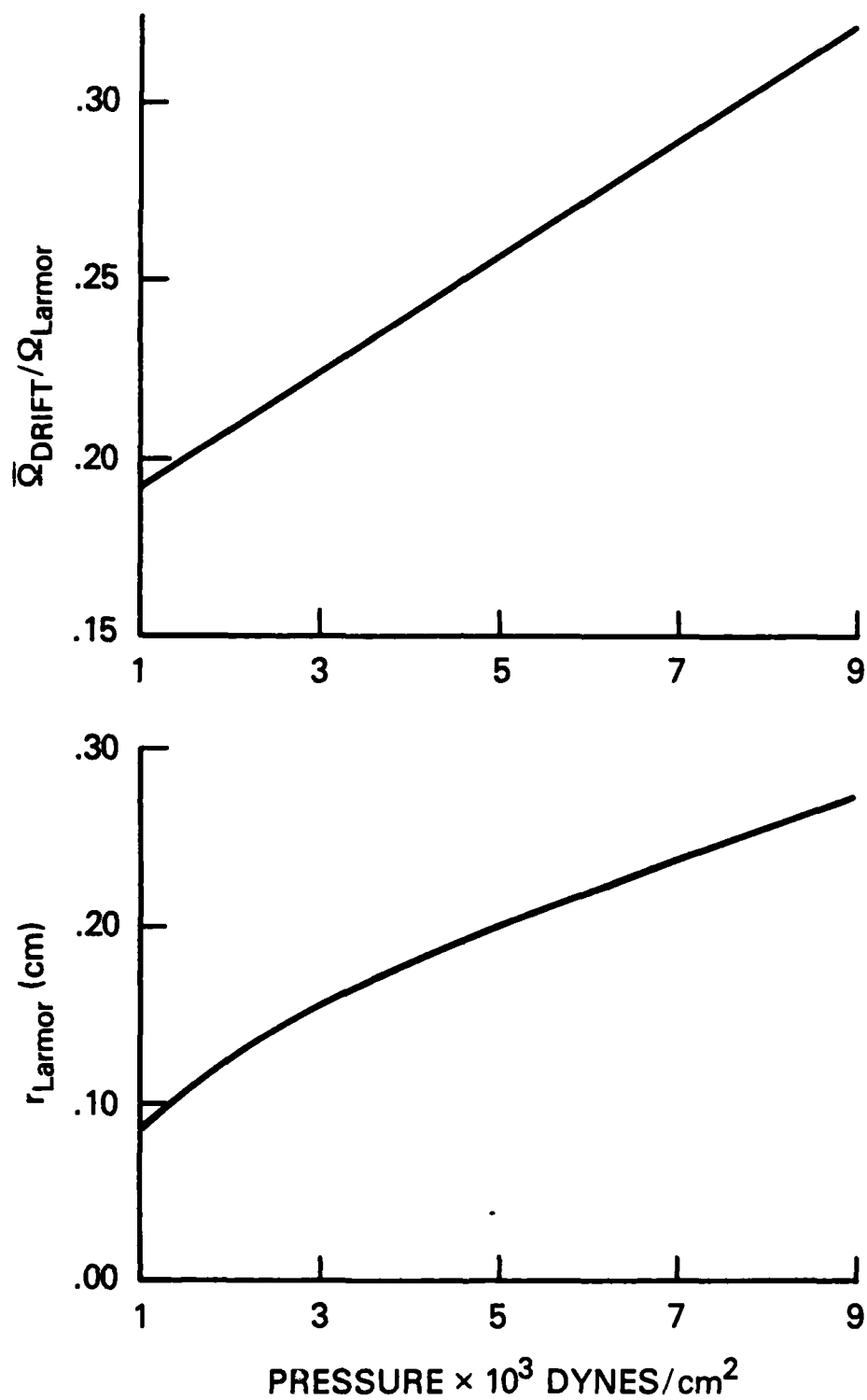


Fig. 3 Poloidal drift and Larmor radius vs. pressure for a 10 kA beam.

$$\Pi_{L-P} = 21.5 \times 10^3 \text{ dynes/cm}^2.$$

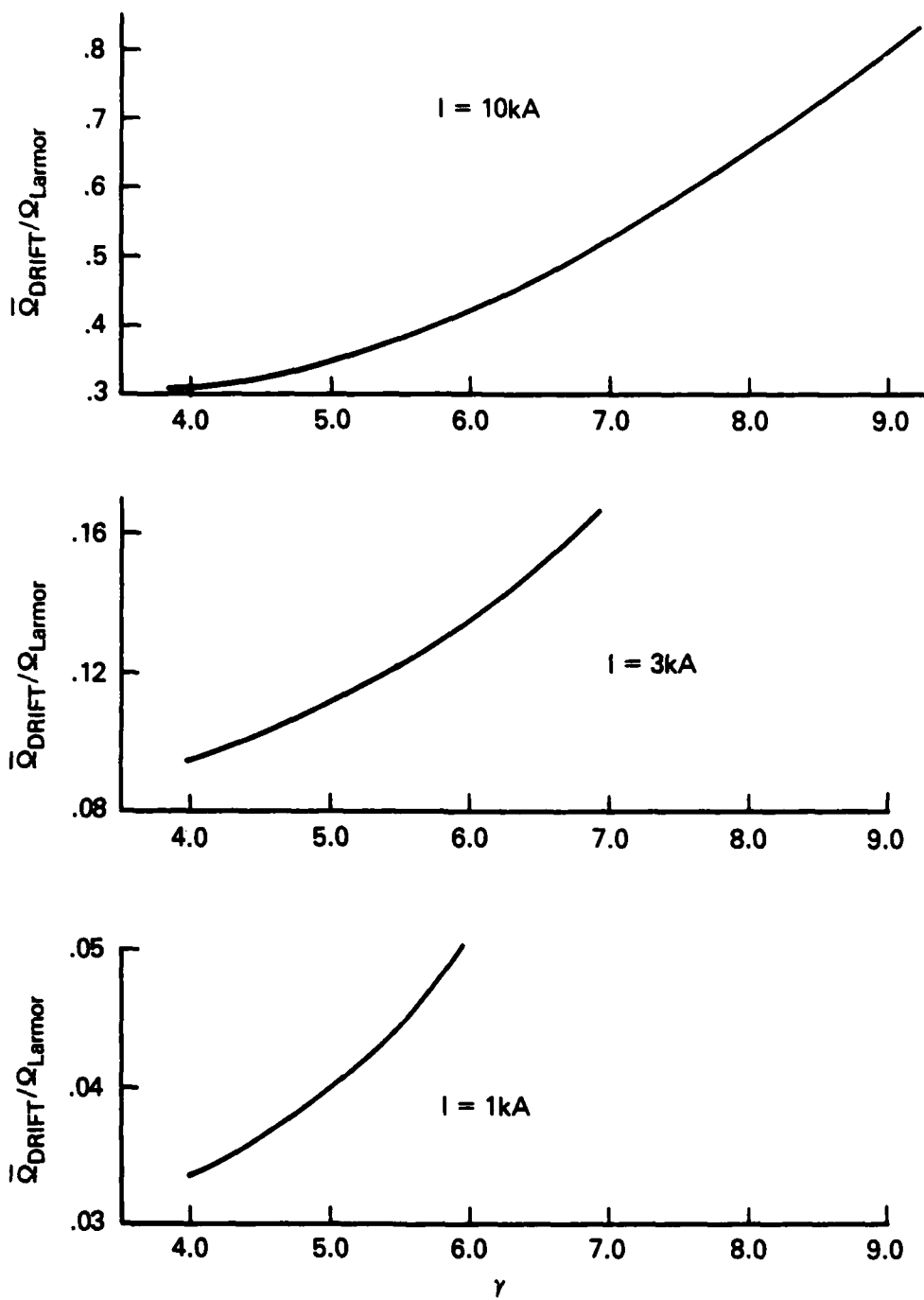


Fig. 4 Poloidal drift during beam acceleration for various injection currents. Initial pressures are 8000, 800 and 100 dynes/cm<sup>2</sup> respectively.

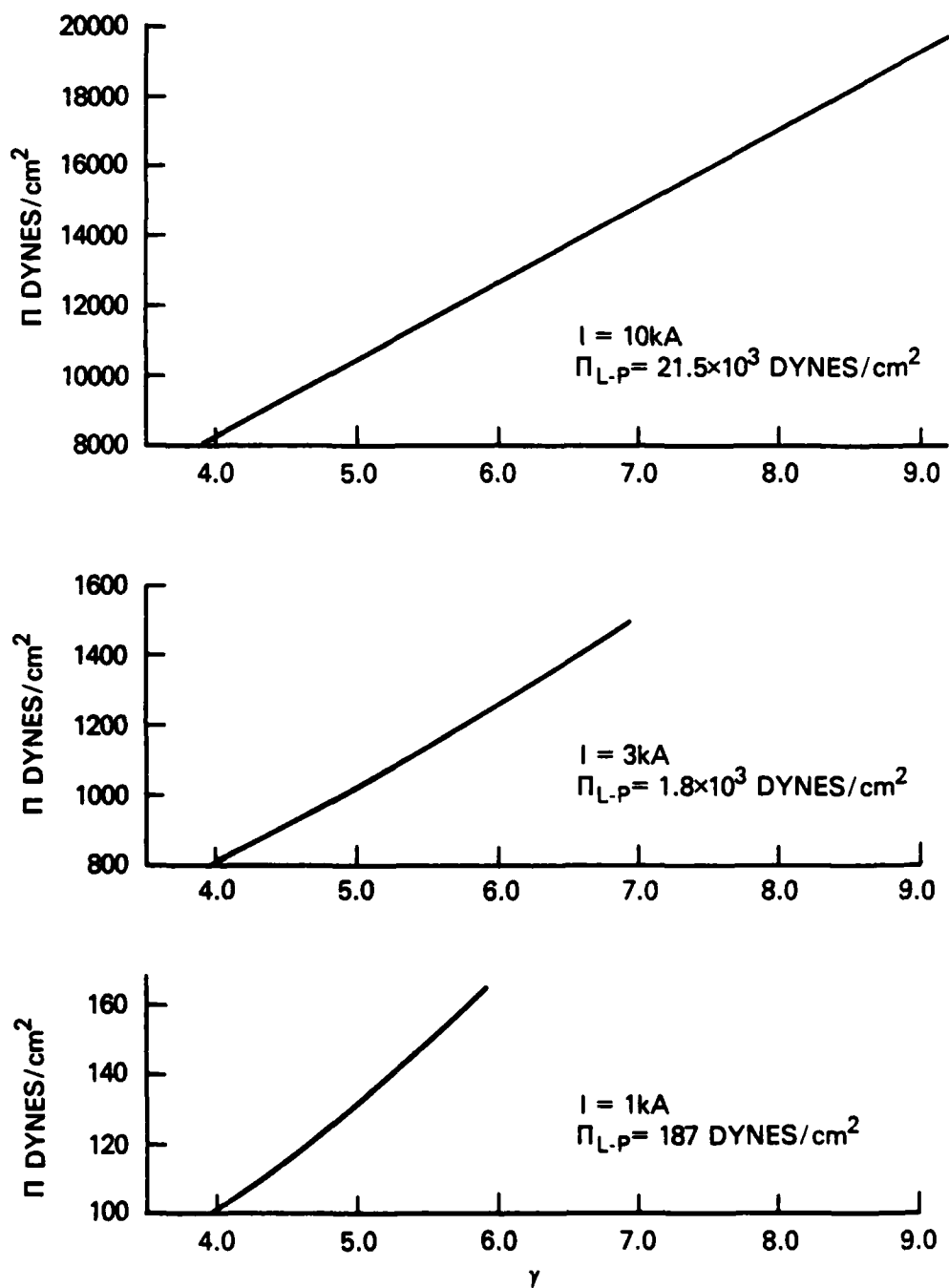


Fig. 5 Peak pressure during acceleration for various injection currents.



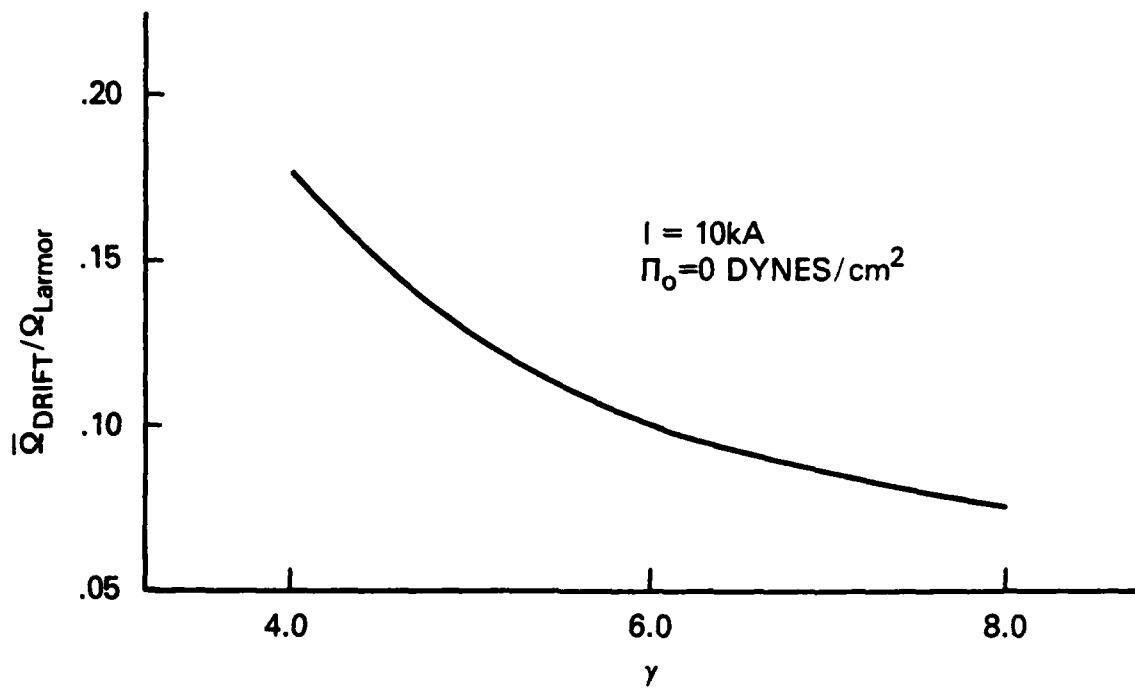


Fig. 6 Poloidal drift during acceleration for a cold beam.  $\bar{\Omega}_{\text{Drift}}$  scales like  $1/\gamma^2$  while  $\Omega_{\text{Larmor}}$  scales like  $1/\gamma$ .

### References

1. N. Rostoker, Particle Accelerators 5, 93 (1973).
2. P. Sprangle and C. A. Kapetanacos, J. Appl. Phys. 49, 1 (1978).
3. N. Rostoker, Comm. Plasma Phys. 6, 91 (1980).
4. C. A. Kapetanacos, P. Sprangle and S. J. Marsh, Phys. Rev. Lett. 49, 741 (1982).
5. C. A. Kapetanacos, P. Sprangle, D. P. Chernin, S. J. Marsh and I. Haber, Phys. Fluids 26, 6 (1983).
6. T. P. Hughes, M. M. Campbell and B. B. Godfrey, Bull. Am. Phys. Soc. 28, 1040 (1983).
7. D. P. Chernin and P. Sprangle, Particle Accelerators 12, 85 (1982).
8. W. M. Manheimer and J. M. Finn, Particle Accelerators 14, 29 (1983).
9. J. M. Finn and W. M. Manheimer, Phys. Fluids 26, 962 (1983).
10. J. M. Grossmann, W. M. Manheimer and J. M. Finn, to be published in Particle Accelerators.
11. W. A. Newcomb, Phys. Fluids 25, 846 (1982).
12. J. D. Dougherty, J. E. Eninger and G. S. Janes, Phys. Fluids 12, 2677 (1969).

## Appendix A: Conservation of Magnetic Moment

To investigate the conservation of the magnetic moment  $\mu$  in the ordering given in Eqs. (7)-(14), we consider the two possible effects that might break the invariance of  $\mu$ . The first is the variation of the relativistic cyclotron frequency  $\omega_c/\gamma$  due to drift motion. That is, we must estimate  $\delta\omega_{cr}/\omega_{cr}$ , where  $\delta$  represents the variation because of guiding center drift into a field inhomogeneity within one relativistic cyclotron period and  $\omega_{cr} = \omega_c/\gamma$ . We first write  $\delta\omega_{cr}/\omega_{cr} = \delta\omega_c/\omega_c - \delta\gamma/\gamma$ . Since  $B_\theta = g(P_\theta)/r$ , we find

$$\left(\frac{\delta\omega_c}{\omega_c}\right)_d \sim \frac{\delta r}{R} \sim \frac{v_d \gamma}{\omega_c R}, \quad (A-1)$$

which is of order  $\epsilon^{3-\delta}$ . ( $\delta r$  is the change in radius  $r$  during one cyclotron period.) Next, using  $\gamma m c^2 + q\phi = E(P_\theta)$ , we find

$$\left(\frac{\delta\gamma}{\gamma}\right)_d \sim \frac{q\delta\phi}{\gamma m c^2} \sim \left(\frac{a}{R} \frac{q\phi}{\gamma m c^2}\right) \left(\frac{v_d \gamma}{\omega_c a}\right), \quad (A-2)$$

where the first of the two factors on the right in (A-2) is due to the relative variation of  $\phi$  along a drift surface due to toroidal effects and the second factor is the angle swept out along the drift surface in one cyclotron period. From  $q\phi/\gamma m c^2 \sim 1/\gamma \sim \epsilon^{1+\delta}$  we see that  $(\delta\gamma/\gamma)_d$  is of order  $\epsilon^4$ .

The other factor which might influence invariance of the magnetic moment is variation of the relativistic cyclotron frequency  $\omega_c/\gamma$  over one gyroradius across the drift surfaces. Again we have two contributing factors, the first of which is

$$\left(\frac{\delta\omega_c}{\omega_c}\right)_g \sim \frac{\delta B_\theta}{B_\theta} = \frac{\delta[g(P_\theta)]}{g(P_\theta)} - \frac{\delta r}{R}. \quad (A-3)$$

The first term is due to the diamagnetic depression from the poloidal beam currents, and the second term is due to the overall  $1/r$  dependence of  $B_\theta$ , i.e.  $B_\theta = g/r$ . We find  $\delta g/g \sim (\Delta g/g)(\rho/a)$ , where  $\Delta g/g$  is the relative depression in self  $B_\theta$  across the whole beam, and is of order  $\epsilon^{2+2\delta}$ . Therefore, we find  $\delta g/g \sim \epsilon^{8/3+2\delta}$ . Also,  $\delta r/R \sim (\rho/a)(a/R) \sim \epsilon^{8/3}$ . Finally, we obtain

$$\left(\frac{\delta\gamma}{\gamma}\right)_g \sim \frac{e\Delta\phi}{\gamma mc^2} \frac{\rho}{a}, \quad (\text{A-4})$$

where the first factor is the drop in electrostatic potential from the center to the edge of the beam, of order  $1/\gamma \sim \epsilon^{1+\delta}$ . Therefore, we find  $(\delta\gamma/\gamma)_g \sim \epsilon^{5/3+\delta}$ .

Summarizing, we find that the total variation  $\delta\omega_{cr}/\omega_{cr}$  over one cyclotron period is dominated by the variation in  $\gamma$  across the drift surface because of the finite Larmor radius of the electrons, and is order  $\epsilon^{5/3+\delta}$ ; this is small for  $\delta$  in the range of interest ( $-1/3 \leq \delta \leq 1/3$ ) so that the magnetic moment is a good invariant.

**END**

**FILMED**

**1-85**

**DTIC**